ELSEVIER

doi:10.1016/j.ultrasmedbio.2009.08.014

● *Technical Note*

THREE-DIMENSIONAL ULTRASOUND GUIDANCE OF AUTONOMOUS ROBOTIC BREAST BIOPSY: FEASIBILITY STUDY

KAICHENG LIANG,* ALBERT J. ROGERS,* EDWARD D. LIGHT,* DANIEL VON ALLMEN,[†]
and STEPHEN W. SMITH*

*Department of Biomedical Engineering, Duke University, Durham, NC; and [†] University of North Carolina School of Medicine, Chapel Hill, NC, USA

Abstract—Feasibility studies of autonomous robot biopsies in tissue have been conducted using real-time three-dimensional (3-D) ultrasound combined with simple thresholding algorithms. The robot first autonomously processed 3-D image volumes received from the ultrasound scanner to locate a metal rod target embedded in turkey breast tissue simulating a calcification, and in a separate experiment, the center of a water-filled void in the breast tissue simulating a cyst. In both experiments the robot then directed a needle to the desired target, with no user input required. Separate needle-touch experiments performed by the image-guided robot in a water tank yielded an rms error of 1.15 mm. (E-mail: kaicheng.liang@duke.edu)   © 2010 World Federation for Ultrasound in Medicine & Biology.

Key Words: **Three-dimensional (3-D) ultrasound, Surgical robotics, Computer aided diagnosis.**

INTRODUCTION

The combination of diagnostic ultrasound (US) scanning with surgical robotics has begun to show promise (SRI International 2005; Leven et al. 2005). Previously we have demonstrated the feasibility of using a real-time three-dimensional (RT3-D) laparoscopic US probe to measure the coordinates of high contrast objects and direct a robot in targeting those objects. We noted the potential use of this system in surgical applications (Pua et al. 2006). The process was later automated using image-thresholding algorithms. The robot was successfully guided to both small hyperechoic targets and large anechoic regions simulating micro-calcifications and cysts respectively in a US phantom using only 3-D US guidance with no human intervention (Whitman et al. 2007). In a subsequent study, the 3-D color Doppler system was tested for the autonomous location of magnetically vibrated ferrous shrapnel (Rogers et al. 2009).

It has been shown that US is a valuable diagnostic tool in breast imaging and is well-suited for enhancing traditional mammography techniques (Carson et al. 1997; Booi et al. 2007; LeCarpentier et al. 2008). Non-RT 3-D

US has been found reliable in verifying the accuracy of typical two-dimensional US-guided core needle breast biopsies (Weismann et al. 2000) and a needle breast biopsy system guided by US has recently been developed, albeit requiring a human operator to manually identify the biopsy location on the scan (Smith et al. 2001).

Percutaneous biopsy of suspicious breast lesions has been found to have diagnostic accuracy similar to that of surgical excision and is now the technique of choice (Hoorntje et al. 2003). Imaging techniques used are largely either stereotactic or US guidance (Liberman et al. 1998). Stereotactic breast biopsy, which uses digital X-ray mammography to localize suspicious regions and is partially automated with the use of a biopsy gun similar to that in prostate biopsy, has a sensitivity comparable to surgical biopsy with specific advantages such as the ability to reach smaller lesions (Schmidt 1994). However the potential use of US as an alternative form of guidance may still be favored for its lack of harmful ionizing radiation typical of X-ray imaging, the possibility of real-time monitoring of the procedure, and the better versatility and cost-effectiveness of US devices over stereotactic equipment (Liberman et al. 1998). The use of automated biopsy guns and vacuum suction to aid sampling from small lesions or thin breasts, are techniques already popular in current clinical practice (Hoorntje et al. 2003), and would be solutions immediately applicable to the potential

Address correspondence to: Kaicheng Liang, Department of Biomedical Engineering, Duke University, Box 99766, Durham NC 27708. E-mail: kaicheng.liang@duke.edu

difficulties of a completely autonomous US-guided procedure. Concerns about movement of tissue during an automated biopsy needle insertion can be addressed with the use of fenestrated compression paddles such as those already designed for stereotactic biopsy (Brenner 2000).

The goal of this article is to examine the feasibility of RT3-D US guidance of an autonomous robotic needle biopsy in excised tissue, *i.e.*, turkey breast with a simulated calcification and a fluid filled cyst. The autonomous robot was successful in both the tasks of contacting the metal tip and targeting the interior of the cyst. These findings are seen as a prelude to animal experiments and investigation into the automation of other typical biopsy procedures.

MATERIALS AND METHODS

The Duke/VMI 3-D scanner (Volumetrics Medical Imaging, Durham, NC, USA) produces a 65° to 90° pyramidal scan at rates up to 30 volumes per s (Smith et al. 1991; von Ramm et al. 1991). The scanner simultaneously displays two B-scans and up to three parallel C-scans at any angle and depth as well as real time 3-D volume rendering, 3-D color and 3-D pulsed Doppler. Each 3-D US scan is comprised of $64 \times 64 = 4096$ B-mode lines, including 512 samples per image line yielding 2 Mbytes of data per 3-D scan. Echo amplitude is eight bits ranging from 0 to 255. For this study we used the commercial VMI transthoracic matrix array that includes 440 transmit channels and 256 receive channels operating at 2.5 MHz previously described by Light et al. (1998). Using parameter values typical in our study, namely wavelength 0.6 mm, depth 50 mm and aperture diameter 12 mm, the voxel spatial resolution of the imaging system is approximately 5.6 mm^3. The beamformer of the imaging system was not adjusted to the sound speed of water and is, thus, a source of error in this study.

The robot used was a Gantry III Cartesian Robot Linear Motion System manufactured by Techno-Isel (Techno, Inc., New Hyde Park, NY, USA) using a Model H26T55-MAC200SD automated controller that accepts input commands and 3-D coordinates from a computer. The XY stage (model HL32SBM201201505) is a stepper motor design providing 340 mm $\times$ 290 mm of travel on a 600 mm $\times$ 500 mm stage. The Z-axis slide (model HL31SBM23051005) provides 125 mm of vertical clearance and allows 80 mm of travel in the z-dimension. As shown in Figure 1a, in this study, the robot was modified such that the Z-axis slide was inclined at a 45° angle (henceforth referred to as the "diagonal" axis) while remaining in the X-Z plane. Thus, we more closely simulated an actual biopsy technique where the biopsy needle typically approaches the target obliquely to avoid the nipple-areola complex as described by Flowers (1998). The biopsy needle (18 G, 15 cm; Cook Medical,
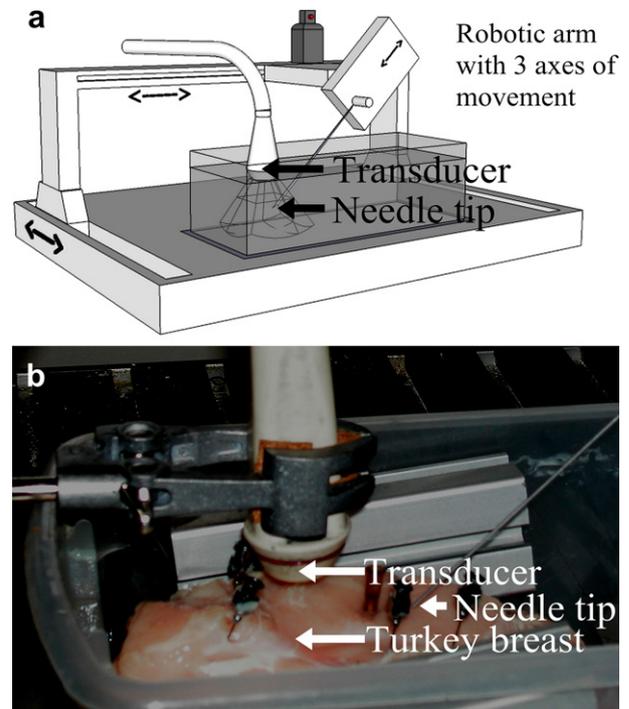

Fig. 1. Schematic (a) and photograph (b) of experimental set-up.

Bloomington, IN, USA) was fixed to the slide such that its movements were controlled by the X-, Y- and diagonal axes of the robot.

The breast phantom used was a boneless turkey breast of variable thickness ranging from 3 cm to 5 cm, which was obtained from a butcher. It was found necessary to remove the loose skin and membranes of the breast as extensively as possible, as trapped air under these structures produced hyperechoic bands on the image, which were misleading to our image segmentation algorithms. To simulate a microcalcification, a metal rod 3 mm in diameter and 10 mm in length was inserted into the thickest part of the breast such that the rod tip was embedded in the center of the thickest cross-section. This microcalcification phantom would be more echogenic and larger than those typical in clinical settings; the mean individual microcalcification size found in one study was 0.29 mm, but microcalcifications were also found expressed in clusters of size 30 mm or larger (Cleverley et al. 1997). To simulate a cyst, a cork borer, 20 mm in diameter, was used to create a void in the breast which was then filled with water. The opening was then plugged with tissue, producing a cyst-like structure of uneven geometry approximately 15 to 20 mm across. The breast was secured to an absorbing rubber base with multiple pins to prevent it from moving during the biopsy, simulating mammogram paddles or the grip of a human operator. Figure 1b shows a photograph of the experimental set-up.

As previously described by Pua et al. (2006) and Whitman et al. (2007), the frame of reference of the robot was zeroed onto a fiducial point, the center spot of the face of a 2.5 matrix array transducer and the physical offset between the transducer face center and the biopsy needle tip was measured. At a user-controlled trigger, a complete 3-D volume of echo data in depth r, azimuth angle θ and elevation angle φ was transmitted, with no user selection of image slices, to a computer running our MATLAB (Mathworks, Natick, MA, USA) image segmentation algorithm. The algorithm then located the desired target defined in Cartesian coordinates. The required Cartesian distances to be traversed by the robot were obtained by subtracting the offset due to the needle tip position. New coordinates were then derived for the robot's diagonal axis configuration, such that X' = X – Z, Y' = Y, and Z' = 1.41Z, where X', Y' and Z' refer to the actual movements of the robot in the X-, Y- and diagonal axes respectively as derived from the Cartesian distances X, Y and Z. The robot then performed the movements and biopsy success was determined by monitoring the real time B- and C-planes of the 3-D scan. Note that sufficient depth of the tissue was ensured such that needle movements in the X- and Y- directions were in water and only in the diagonal axis did the needle eventually make contact with and penetrate the tissue. This process not only prevents the cyst structure being altered from the initial geometry that was imaged; it can help minimize unnecessary and potentially painful tissue distortion for the patient except what is absolutely necessary for the needle biopsy.

The segmentation algorithm for the microcalcification, previously described by Whitman et al. (2007), located calcifications in a 3-D US image by selecting voxels of amplitude above a preset threshold and rejecting voxels below this threshold. To measure the targeting error of our robot, a needle-touch experiment was performed, where a needle tip immersed in a tank of water was used as a target for the biopsy needle and located using the calcification algorithm. After each attempted target engagement by the biopsy needle, error was measured by first manually jogging the robot in 0.1 mm steps in all three axes until both needle tips were touching and then calculating the magnitude of the error vector using trigonometry. Five trials were performed and after each attempt, the target was repositioned. Note that analogous error measurements were not possible once the biopsy needle was embedded in the tissue samples. For the experiment of locating the simulated calcification in the turkey breast, five trials were performed and the breast was repositioned each time.

The segmentation algorithm for detection of a cyst in a 3-D US scan, previously described by Whitman et al. was used with modifications as follows. First, analogous thresholding was performed, such that all voxels whose amplitude fell above a preset threshold were rejected. Next, voxels that remained and did not have neighbors within a 1 mm radius were rejected, to remove both image noise and amplitude minima in the speckle assumed to lie within contiguous tissue. To clean up remaining extraneous noise, the mean distance of all the remaining voxels from the approximate center of the remaining image volume (found by taking an arithmetic mean of the voxels in each axis) was calculated and voxels more than half this distance away from the approximate center were rejected. The center of the remaining voxels, approximated by again taking an arithmetic mean in each axis, was then designated as the desired target of the biopsy needle. Five cyst biopsy trials were performed and the breast was repositioned for each trial.

RESULTS

The rms error for the needle-touch experiment in a water tank was 1.15 mm, amounting to a 1.45% error relative to the total travel distance of the needle in all three axes. Table 1 presents the total travel distances and relevant error measurements. This error is comparable to and may be an improvement over the placement error of existing stereotactic biopsy systems which has been quoted as 2 mm (Schmidt 1994). Since the mean depth of microcalcifications beneath the skin surface is known to range from 6 to 30 mm (Cleverley et al. 1997), the parameters of our study lie within clinical expectations and thus the comparison of placement error is appropriate.

Figure 2 shows a typical result of the simulated calcification biopsy comparing simultaneous perpendicular image planes of the rod tip before (Figs. 2a–c) and during (Fig. 2d–f) the biopsy. Figure 2d–f show the needle tip about to make contact with the target. The snapshots were taken at the instant before the needle touched the rod tip, for the two to be physically discernible in the scans. In all five trials, the biopsy needle made contact squarely on the rod tip and could be seen displacing the rod tip.

Figure 3 illustrates the results of the simulated cyst biopsy. Figure 3a shows a real-time 3-D rendered image of the breast including the cyst, which typifies the scan volume automatically transmitted to the computer for processing. Figure 3b shows a single cross-section through

Table 1. Total travel distances and errors in needle-touch experiment

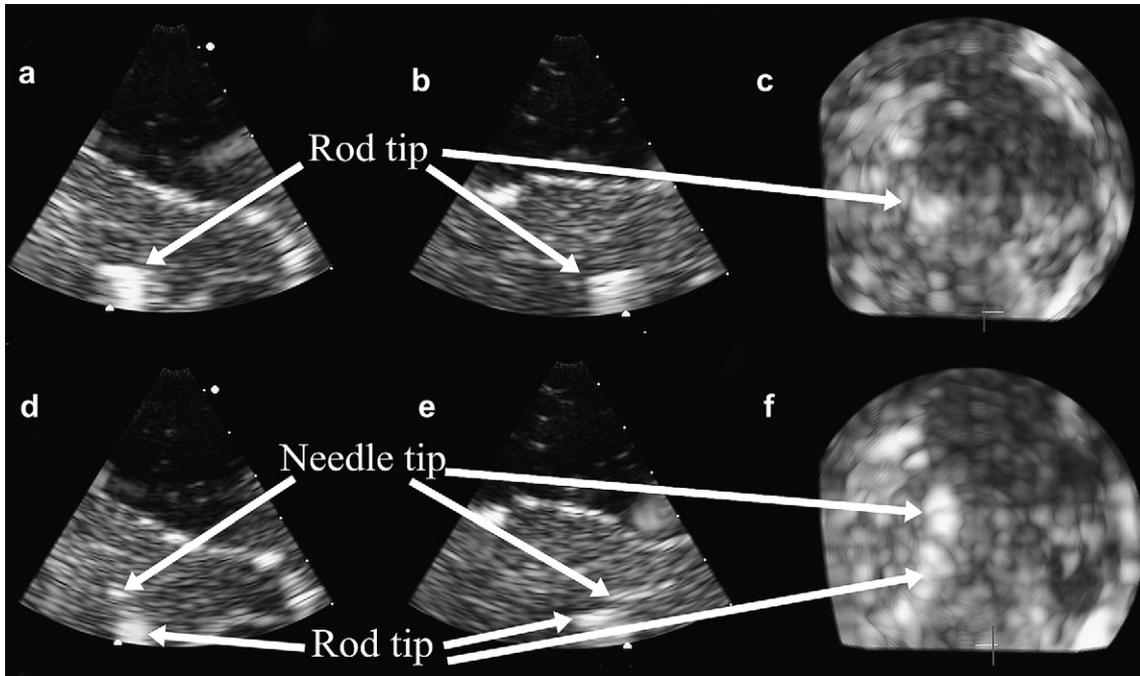| Total travel distance/mm	Error/mm
83.3	1.63
88.0	0
78.3	1.14
75.1	1.27
72.6	1.01
Mean = 79.5	rms error = 1.15

Fig. 2. (a), (b) and (c) show the simultaneous B-scans and C-scan respectively of the simulated calcification in turkey breast before needle approach. (d), (e) and (f) show the corresponding scans of the approaching biopsy needle.

the volume for illustration purposes only. Figure 3(c-e) show simultaneous B- and C-mode planes demonstrating that the biopsy needle successfully penetrated the cyst and the needle tip reached the interior of the cyst. The cyst was successfully targeted in each of the five trials.

DISCUSSION

We have further extended our demonstration of the feasibility of an autonomous robot performing simple surgical tasks under the guidance of RT3-D US imaging
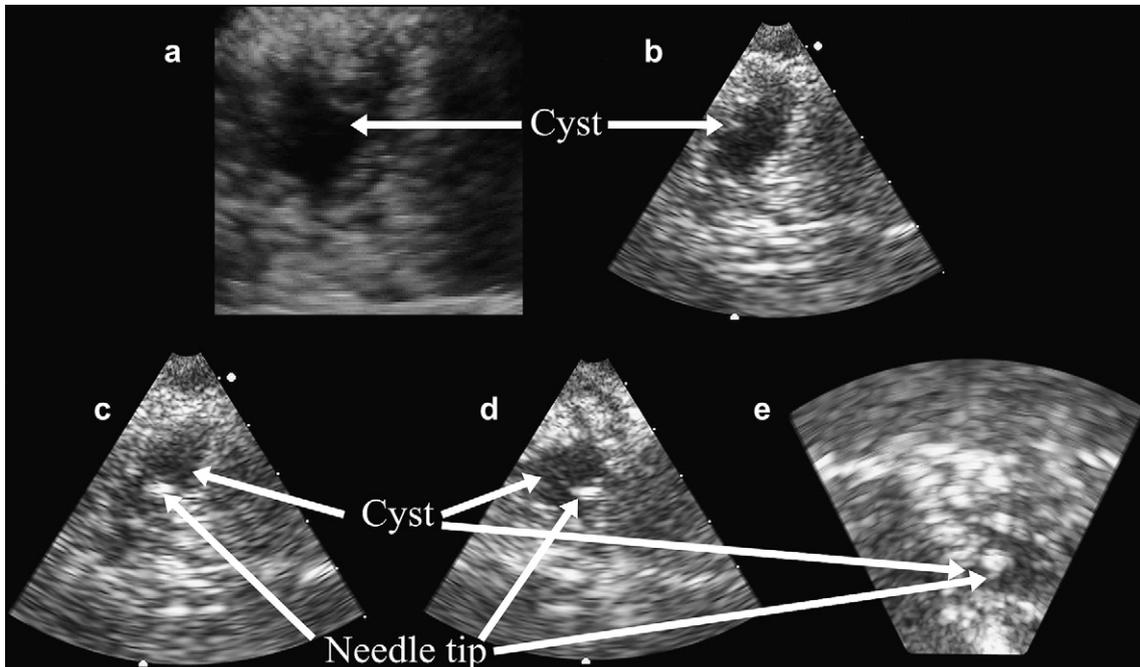

Fig. 3. (a) shows a three-dimensional (3-D) rendered image of the cyst in turkey breast and (b) is a B-scan of the cyst. (c), (d) and (e) are the simultaneous B-scans and C-scan, respectively, of the needle tip penetrating the cyst.

and simple image processing algorithms. Error is due to (1) the limited spatial resolution of the scanner, (2) the beamformer not adjusted to the sound speed of water, (3) the alignment of the robot's frame of reference with that of the transducer to obtain accurate voxel coordinates and (4) the relatively unsophisticated image segmentation algorithms used. More advanced segmentation algorithms for 3-D US data have been proposed but the amplitude thresholding used in this study remains an important step in these more elaborate processes (Boukerroui et al. 2001; Horsch et al. 2002). We chose to use the simplest possible algorithm to optimize computation speed and it is also a useful foundation for the implementation of more intensive image analysis. Computer aided diagnosis of breast lesions using more sophisticated algorithms to analyze breast US data is an area of active development (Horsch et al. 2002).

The most significant limitation of this study was the lengthy time required for scan volume transfer and the processing of the image volume. From the start of the volume acquisition till the successful targeting by the biopsy needle, the calcification biopsy took just under a minute and the cyst biopsy took approximately 3 min. However, more sophisticated data transmission protocols and algorithms written with more efficient computing languages would reduce that time by at least an order of magnitude. Typical US probes used in breast biopsies are 7 to 12 MHz as noted by Flowers (1998), which would yield images of far higher contrast and spatial resolution than those in our study. A robot arm with increased degrees of freedom would also shorten the required movement time of the needle to reach its desired location. Finally, the RT3-D color Doppler features of the volumetric scanner may offer capabilities in targeting or avoiding blood vessels.

CONCLUSION

We have developed and tested the feasibility of an RT3-D US guided robotic system that can autonomously locate both simulated calcifications and cysts in tissue with high repeatability and accuracy. By simulating simple procedures common in typical breast biopsies, this study has demonstrated that autonomous guidance might eventually be extended to many relatively straightforward surgical tasks performed in large volume at hospitals and clinics.

REFERENCES

Booi RC, Krucker JF, Goodsitt MM, O'Donnell M, Kapur A, LeCarpentier GL, Roubidoux MA, Fowlkes JB, Carson PL. Evaluating thin compression paddles for mammographically compatible ultrasound. Ultrasound Med Biol 2007;33:472–482.

Boukerroui D, Basset O, Baskurt A, Gimenez G. A multiparametric and multiresolution segmentation algorithm of 3-D ultrasonic data. IEEE Trans Ultrason Ferroelectr Freq Control 2001;48:64–77.

Brenner RJ. Lesions entirely removed during stereotactic biopsy: Preoperative localization on the basis of mammographic landmarks and feasibility of freehand technique-initial experience. Radiology 2000;214:585–590.

Carson PL, Moskalik AP, Govil A, Roubidoux MA, Fowlkes JB, Normolle D, Adler DD, Rubin JM, Helvie M. The 3-D and 2D color flow display of breast masses. Ultrasound Med Biol 1997;23:837–849.

Cleverley JR, Jackson AR, Bateman AC. Preoperative localization of breast microcalcification using high-frequency ultrasound. Clin Radiol 1997;52:924–926.

Flowers C, Ultrasound guided core biopsy. In: Flowers C, (ed). Image guided core biopsy of the breast: A practical approach. London: Greenwich Medical Media; 1998. p. 21–28.

Hoorntje LE, Peeters PHM, Mali WPTM, Rinkes IHMB. Vacuum-assisted breast biopsy: A critical review. Eur J Cancer 2003;39:1676–1683.

Horsch K, Giger ML, Venta LA, Vyborny CJ. Computerized diagnosis of breast lesions on ultrasound. Med Phys 2002;29:157–164.

LeCarpentier GL, Roubidoux MA, Fowlkes JB, Krucker JF, Hunt KA, Paramagul C, Johnson TD, Thorson NJ, Engle KD, Carson PL. Suspicious breast lesions: Assessment of 3-D Doppler US indexes for classification in a test population and fourfold cross-validation scheme. Radiology 2008;249:463–470.

Leven JBD, Kumar R, Zhang G, Blumenkranz S, Dai XD, Awad M, Hager GD, Marohn M, Choti M, Hasser C, Taylor RH. DaVinci canvas: A telerobotic surgical system with integrated, robot-assisted, laparoscopic ultrasound capability. Med Image Comput Comput Assist Interv Int Conf 2005;3749:811–818.

Liberman L, Feng TL, Dershaw DD, Morris EA, Abramson AF. US-guided core breast biopsy: Use and cost-effectiveness. Radiology 1998;208:717–723.

Light ED, Davidsen RE, Fiering JO, Hruschka TA, Smith SW. Progress in 2-D arrays for real-time volumetric imaging. Ultrason Imaging 1998;20:1–16.

Pua EC, Fronheiser MP, Noble J, Light ED, Von Allmen D, Smith SW. 3-D Ultrasound guidance of surgical robotics: A feasibility study. IEEE Trans Ultrason Ferroelectr Freq Control 2006;53:1999–2008.

Rogers AJ, Light ED, Smith SW. 3-D ultrasound guidance of autonomous robot for location of ferrous shrapnel. IEEE Trans Ultrason Ferroelectr Freq Control 2009;56:1301–1303.

Schmidt RA. Stereotactic breast biopsy. CA Cancer J Clin 1994;44:172–91.

Smith SW, Pavy HE, von Ramm OT. High speed ultrasound volumetric imaging system part I: Transducer design and beam steering. IEEE Trans Ultrason Ferroelectr Freq Control 1991;38:100–108.

Smith WL, Surry KJM, Mills GR, Downey DB, Fenster A. Three-dimensional ultrasound-guided core needle breast biopsy. Ultrasound Med Biol 2001;27:1025–1034.

SRI International. DARPA Selects SRI International to Lead Trauma Pod Battlefield Medical Treatment System Development Program. March 28, 2005. Available at: http://www.sri.com/news/releases/03-28-05.html. Access date: April 1, 2009.

von Ramm OT, Smith SW, Pavy HE. High speed ultrasound volumetric imaging system part II: parallel processing and display. IEEE Trans Ultrason Ferroelectr Freq Control 1991;38:109–115.

Weismann CF, Forstner R, Prokop E, Rettenbacher T. Three-dimensional targeting: A new three-dimensional ultrasound technique to evaluate needle position during breast biopsy. Ultrasound Obstet Gynecol 2000;16:359–364.

Whitman J, Fronheiser MP, Ivancevich NM, Smith SW. Autonomous surgical robotics using 3-D ultrasound guidance: Feasibility study. Ultrason Imaging 2007;29:213–219.